1978ARA&A..16..429S

Ann. Rev. Astron. Astrophys. 1978. 16:429–43
Copyright © 1978 by Annual Reviews Inc. All rights reserved

*2137

A VIEW OF SOLAR MAGNETIC FIELDS, THE SOLAR CORONA, AND THE SOLAR WIND IN THREE DIMENSIONS

Leif Svalgaard and John M. Wilcox
Institute for Plasma Research, Stanford University,
Stanford, California 94305

1 INTRODUCTION

In the last few years we have learned that the solar corona and the solar wind are three-dimensional. That is, the deviations from spherical or even cylindrical symmetry are first-order effects, which are important for our basic description and indeed physical understanding of the coronal expansion. The recognition of this simple fact has been a slow process, perhaps because it complicates the mathematical treatment. Even a quick look at the solar corona reveals a highly structured medium with large density gradients. For almost a century (Bigelow 1889) it has been suggested that magnetic fields are the fundamental agent that controls the shape of the corona and determines the inner boundary conditions for the solar wind escape. Only recently have we recognized how *dominant* is the role of large-scale magnetic fields in determining the global structure of the solar wind. The highly successful "SKYLAB Workshop on Coronal Holes" that was conducted last year has been important for the general acceptance of the new three-dimensional description of the structure of the corona and the interplanetary magnetic field. Zirker (1977) and Hundhausen (1977) have aptly summarized the insight resulting from this work. The present review is a further synthesis based on a broader data base than that available to the Workshop. We attempt to provide a unified viewpoint recognizing that such an attempt is usually associated with a certain degree of oversimplification.

0066-4146/78/0915-0429$01.00

© Annual Reviews Inc. • Provided by the NASA Astrophysics Data System

1978ARA&A..16..429S

2 MODELS OF CORONAL MAGNETIC FIELDS

The recent empirical clarification of coronal and interplanetary phenomenology has not yet been matched by a similar advance in our physical understanding of the processes giving rise to the solar wind. Some time ago, Pneuman & Kopp (1971) and also Endler (1971) obtained numerical solutions to the MHD-equations for an isothermal coronal plasma in a solar magnetic field assumed to be a dipole at the base of the corona. Figure 1 shows the magnetic field geometry computed by Pneuman and Kopp. The flow streamlines coincide with the magnetic field lines. The pressure of the coronal plasma dominates at higher latitudes, forcing the opening of field lines and permitting expansion of the plasma. Some closed field lines remain near the equator. Even these closed field lines are somewhat distended by the plasma pressure. This field geometry is nearly identical to the "current sheet model" developed by Schatten (1971a) to compute coronal and interplanetary field geometries. A current sheet must flow along the boundary of the closed region and in the equatorial plane in the open region to maintain pressure balance.

This oversimplified physical model does strikingly illustrate a number of points that are crucial to our present empirical understanding of the geometry of the coronal magnetic field and of the coronal expansion. The solar wind flows along the open magnetic field lines from higher latitudes, while a band along the equator is characterized by closed magnetic fields with no solar wind expansion. In the open regions, the field lines spread out faster than radially, while in the equatorial plane they are separated by an equatorial current sheet encircling the Sun.

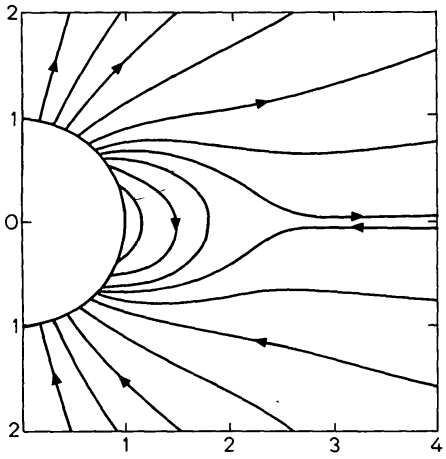

Figure 1 The magnetic field line configuration (Pneuman & Kopp 1971) for equilibrium of an isothermal corona with a dipole magnetic field imposed at the solar surface. The direction of the field is shown as was typical of the present sunspot minimum.

© Annual Reviews Inc. • Provided by the NASA Astrophysics Data System

1978ARA&A..16..429S

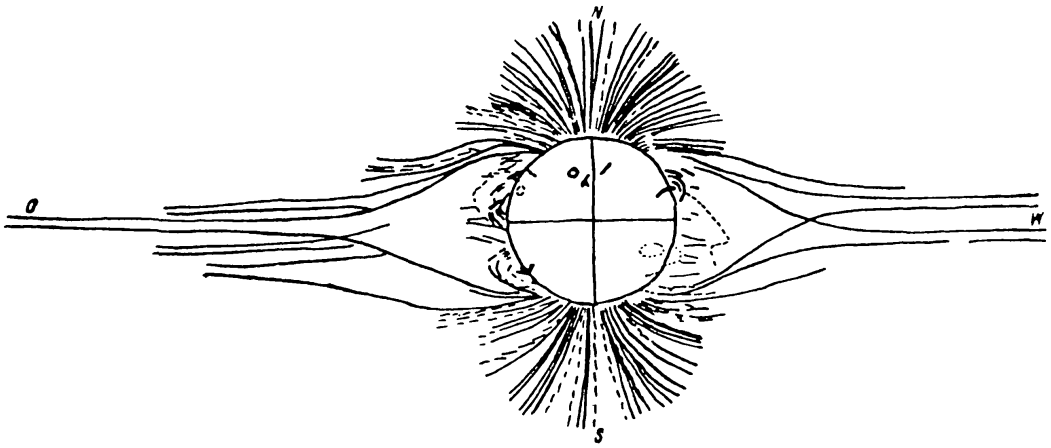

Figure 2 Drawing of the corona at the June 30, 1954 eclipse near sunspot minimum. This drawing clearly shows how the structures extend to lower heliographic latitudes with increasing radial distance (Vseskhsvjatsky 1963).

Although the Pneuman and Kopp computation refers to a highly idealized situation, the real corona sometimes does resemble the field geometry shown in Figure 1. An example is shown in Figure 2, a drawing of the famous "minimum-corona" of 1954.

Computations by several workers [e.g. Schatten et al. (1969), Altschuler & Newkirk (1969), Levine (1977), Schatten (1976), and subsequent verification by Waldmeier (1977), and Riesebieter (1977)] have repeatedly shown that the observed field-line geometry in the corona within about three solar radii can be closely approximated by a potential magnetic field given by a specified field at the base of the corona supplemented by the assumption that the expansion of the solar wind can be simulated by specifying an outer equipotential spherical surface, at which all magnetic field lines become radial. This so-called "source surface" is usually assumed to be located at about two solar radii from the center of the Sun; the estimates range from 1.6 to 2.6 solar radii. A simple consequence of the potential assumption is a considerable simplification of the coronal structure with height over the solar surface. The influence of smaller-scale features (or "higher harmonics") diminishes more rapidly with altitude than that of the large-scale ("low order") structures, resulting in an increasing dominance of the latter at greater heights.

3 LARGE-SCALE SOLAR STRUCTURE

As an example of the simplification mentioned in the previous section, consider the situation around the time of the sunspot minimum we have just passed. Figure 3 shows an average synoptic map of the line-of-sight

© Annual Reviews Inc. • Provided by the NASA Astrophysics Data System

1978ARA&A..16..429S

photospheric magnetic field as it was observed at the Stanford Solar Observatory during the past year. The Stanford magnetograph has been discussed by Scherrer et al. (1977) and by Duvall (1977). The aperture of the magnetograph is three minutes of arc corresponding to a spatial resolution comparable with order 12 in the spherical harmonic expansion of the magnetic potential. Solid contour lines show fields directed outward from the Sun (positive fields), while dashed lines indicate fields directed into the Sun (negative fields). The map is fairly complex despite the fact that it is a time average extending over more than a year. However, a large-scale pattern consisting of an axial dipole (positive fields in the northern polar cap; negative in the southern) plus an equatorial quadrupole (i.e. four polarity reversals around the equator) can be discerned. Inspection of individual rotations reveals the persistence of this basic pattern throughout the interval.

The map in Figure 3 may now be used as the inner boundary condition in a spherical harmonic expansion of the magnetic potential. Plots of the fields generated from the expansion are shown in Figure 4. Had we retained all harmonics we would reproduce Figure 3. In order to accentuate the large-scale structure we show in the upper panel of Figure 4 the surface fields generated from coefficients through order four only. We compute and plot here the radial component of the magnetic field. The neutral-line winds its way across the solar surface delineating four equatorial regions [or "sectors," Svalgaard et al. (1975), Wilcox (1971)] of alternating polarity. These photospheric sectors extended up to about 45° latitude on both sides of the equator. In the middle panel of Figure 4 we show the neutral line on a surface 1.4 $R_\odot$ from the Sun's center or 0.4 $R_\odot$ above the photosphere.

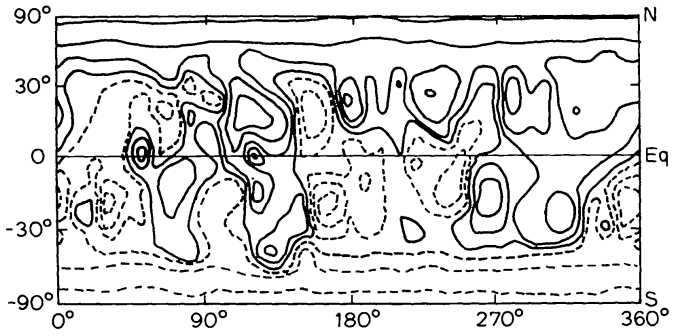

Figure 3 Average synoptic map of the line-of-sight photospheric magnetic field covering eighteen 27^d rotations starting May 5, 1976 and ending August 7, 1977. Because the recurrence period of the interplanetary magnetic field was very close to 27^d during this interval, a 27^d calendar was used rather than the usual 27.3^d Carrington rotation system. Positive contours are shown as solid lines at 0, +0.2, +0.5, +1, and +2 G, while negative contours (−0.2, −0.5, ...) are shown as dashed lines. The positive field direction is away from the Sun or outwards (i.e. towards the observer).

© Annual Reviews Inc. • Provided by the NASA Astrophysics Data System

1978ARA&A..16..429S

The structure has become even simpler up here and in addition the latitudinal extent of the sectors has decreased to about 30°. Finally, in the lower panel of Figure 4, we show the computed neutral line on the source surface, 2.6 solar radii from the center of the Sun. The excursion in latitude has decreased further (varying from 5° to 30° depending on sector), and the neutral line is now only gently warped. Retaining all 12 orders in the spherical expansion leads to virtually the same neutral-line geometry on the source surface as shown here, demonstrating the dominance of the large-scale features.

The effect of the axial dipole component is effectively to decrease the latitudinal extent of any azimuthal organization, such as sectors, with altitude. This effect is clearly illustrated in Figure 5, which shows the neutral-line location on the source surface for varying strength of the dipolar component. The center panel of Figure 5 is identical to the lower panel of Figure 4 corresponding to the actual observed polar fields (with the low resolution of 3′). Doubling the polar fields has the result shown in the top panel of Figure 5: the latitudinal excursion of the warped neutral line is greatly reduced, while decreasing the polar fields by a factor of two results in a greater latitudinal range of the neutral line (lower panel of Figure 5). We see here how sensitive is the latitudinal excursion of the neutral line to the magnetic flux through the polar caps. This latter quantity is thus of fundamental importance for the structure of coronal and hence interplanetary magnetic fields.

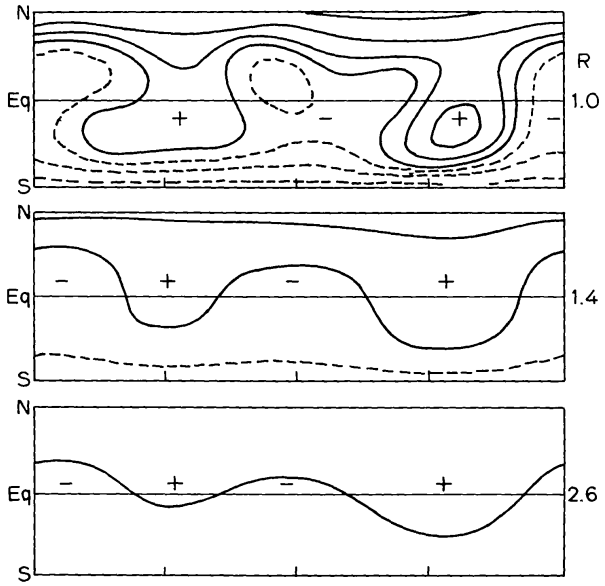

Figure 4 Computed radial component of the magnetic field of the Sun using the observed line-of-sight field of Figure 3 as the inner boundary condition and setting the radius of the source surface equal to 2.6 solar radii. The contours are drawn at ±0.2, ±0.5, ±1 G, while the neutral line is drawn as a heavy line. The three synoptic maps show the field on surfaces at 1.0 $R_\odot$ (top), 1.4 $R_\odot$ (middle), and 2.6 $R_\odot$ (bottom) heliocentric distance.

© Annual Reviews Inc. • Provided by the NASA Astrophysics Data System

1978ARA&A..16..429S

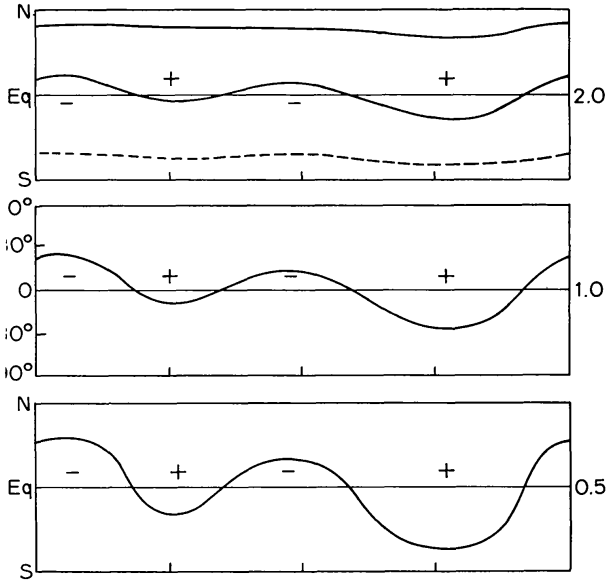

Figure 5 Computed neutral lines on a source surface at 2.6 solar radii for different values of the strength of the axial dipole. The center panel is identical to the lower panel of Figure 4. Doubling the axial dipole strength depresses the latitude of the maximum excursions of the neutral line as shown in the top panel. With polar fields only half as strong we get the lower panel.

4 INTERPLANETARY MAGNETIC FIELD

Extending radially outwards from the neutral line on the source surface we find the warped current sheet that separates opposite magnetic polarities in interplanetary space. As the Earth—and spacecraft near the ecliptic plane—is within $\pm 7°$ of the solar equatorial plane, the warps in the current sheet are normally large enough so that as the Sun rotates, the current sheet will overtake the almost stationary Earth four times every 27 days. The polarity of the interplanetary magnetic field will thus change four times, and four so-called sector boundaries would have been observed to sweep past the Earth (Wilcox & Ness 1965). We see now that in reality there is only *one* "sector boundary" in interplanetary space: the warped current sheet that separates positive and negative magnetic fields (Schulz 1973).

The warps are caused by a sector-like organization of low-latitude magnetic fields in the photosphere with essentially north-south boundaries between polarities. With increasing distance from the Sun, the polar fields depress the sectors to lower and lower latitudes. In extreme cases—i.e. if a magnetic sector is weak or deformed by active regions, its corresponding warp may be very small or even absent. On the other hand, at times just after sunspot maximum, when the polar fields weaken and

© Annual Reviews Inc. • Provided by the NASA Astrophysics Data System

1978ARA&A..16..429S

reverse polarity, the sector warps may—and very likely do—extend to very high heliographic latitudes and become dominant in the interplanetary medium (Schatten 1971b). Figure 6 shows a schematic of the warped sector boundary surface as it is curved by solar rotation into a spiral shape. Solid lines show where the surface curves above the solar equatorial plane, and dashed lines show where the current sheet, flowing in the surface, warps below the equatorial plane (Svalgaard & Wilcox 1976). On its way to Saturn, Pioneer 11 in February 1976 went 16° north of the ecliptic plane and for several months observed an interplanetary magnetic field almost entirely away from the Sun (Smith et al. 1978), while at the same time a distinct sector structure of alternating polarities was observed at the Earth. What happened was simply that the spacecraft got so far above the equatorial plane that the sector boundary did not reach it. Occasionally that happens even to the Earth itself, most notably in 1954 (e.g. Antonucci 1974).

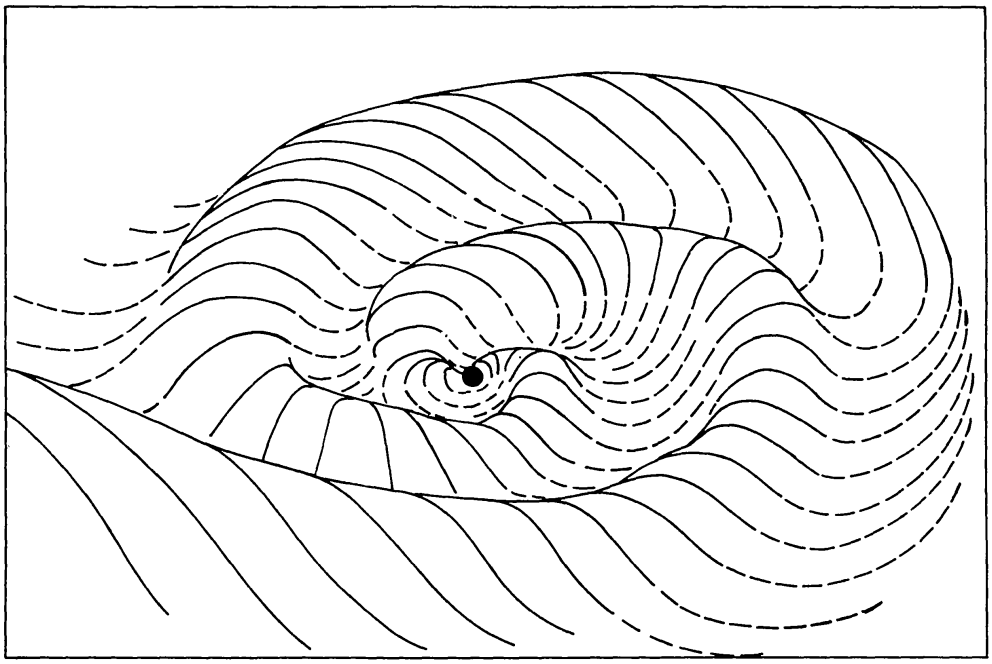

Figure 6 Sketch showing the warped current sheet in the inner solar system (inside of 6 au). This current sheet divides the interplanetary magnetic field in the heliosphere into two regions with oppositely directed field lines. In one region the field polarity is away from the Sun (at present this region is north of the solar equator), in the other region the field polarity is toward the Sun. The situation is shown for a four-sector structure and we try to depict the shape of a surface in three dimensions. Where this surface—in which the current flows—lies above the solar equatorial plane it is shown by full lines, while dashed lines indicate that the current sheet dips below the equatorial plane. The extent in latitude of the current sheet was assumed to be $\pm 15°$. The Sun at the center is not to scale (from Svalgaard & Wilcox 1976).

© Annual Reviews Inc. • Provided by the NASA Astrophysics Data System

1978ARA&A..16..429S

5 CORONAL HOLES

Close to the Sun the warps induced by the sector structure can be very significant. Figure 7 shows schematically how the region of closed field lines just below the current sheet—at the base of the current—winds across the solar surface. In this region the plasma is trapped and the density is correspondingly higher. The white-light corona is thus brighter in this region. As a matter of fact, Figure 7 shows the three-dimensional structure of enhanced white-light corona as deduced from observations with the OSO-7 coronograph by Howard & Koomen (1974), who found this structure to be well correlated with the sector structure of the interplanetary magnetic field as suggested by Hansen et al. (1974) and by Svalgaard et al. (1974). This band of bright corona delineates the sector boundary near the Sun.

Away from this band the corona can be quite dark in the absence of solar activity. Such low-brightness (i.e. low-density) regions are known as coronal holes and are often found in the polar caps and in the middle of magnetic sectors (e.g. Wilcox & Svalgaard 1974). Bohlin (1977) has constructed an excellent one-line definition for a coronal hole: "a fairly

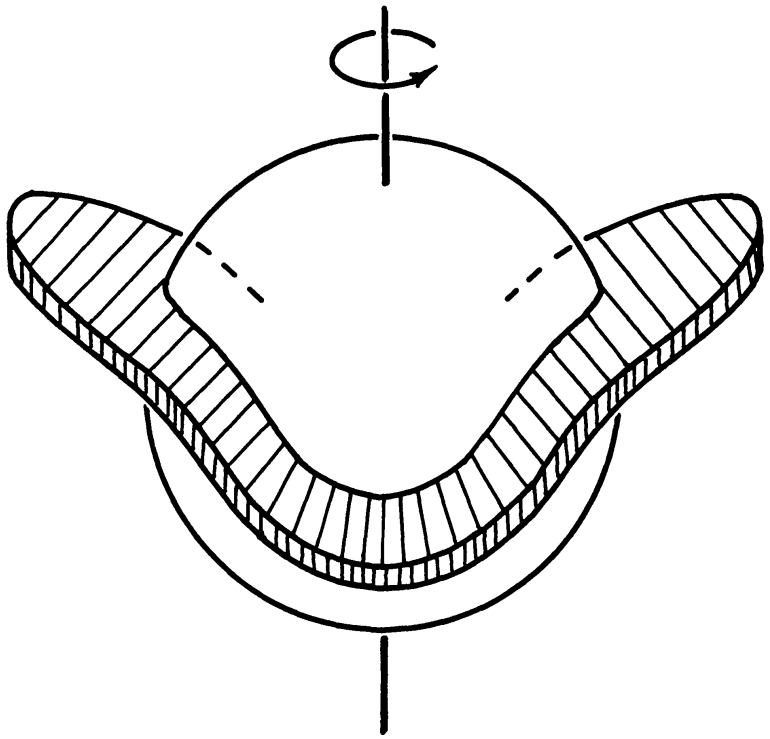

Figure 7 Schematic of coronal structure consistent with observations by Howard & Koomen (1974) of correlation between brightness (and thus density) enhancements and sector structure.

© Annual Reviews Inc. • Provided by the NASA Astrophysics Data System

1978ARA&A..16..429S

large-scale cool low-density area in the corona encompassing weak, predominantly unipolar magnetic fields which extend away from the Sun in diverging open lines of force, that give rise to high-speed solar wind streams that cause geomagnetic activity."

Maybe as important as the formation of a coronal hole within a magnetic sector is the persistent warp in the current sheet that is caused by the sector. This warp is there as long as the magnetic sector exists [which may well be decades or longer; see Svalgaard & Wilcox (1975)], whether or not the sector is occupied by a coronal hole. In this view coronal holes are accidental *effects* of conditions pertaining to the large-scale magnetic configuration rather than being fundamental constructs themselves. The influence of holes can be quite dramatic, however. Figure 8 shows a synoptic map of the coronal brightness during mid-1974 in the upper panel. The neutral line or sector boundary is well marked by the winding contours of bright corona. At this time there were two sectors per rotation. Low-density regions extend to and even across the equator from both polar caps. The observed solar-wind speed and magnetic polarity at the Earth are shown in the lower panel with due allowance for the transit time of the plasma from the Sun to the Earth. That is, the solar wind properties have been transferred to their likely

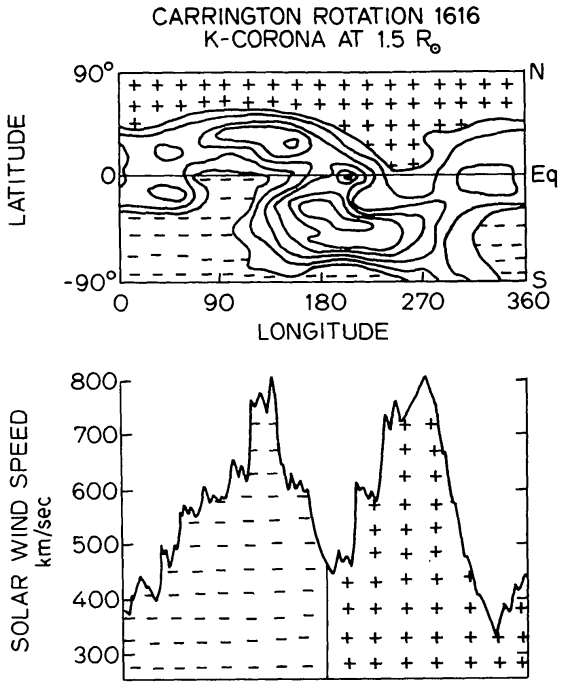

Figure 8 K-Coronal brightness contour map for Carrington rotation 1616 in mid-1974 and observed solar wind speed and magnetic polarity variations with estimated Carrington source longitude. (After Hundhausen 1977). The two high-speed streams are assumed to originate in regions on the Sun marked by the same polarity as the stream.

© Annual Reviews Inc. • Provided by the NASA Astrophysics Data System

1978ARA&A..16..429S

source longitude. The solar wind speed reaches very high values ($\cong$800 km sec^{-1}) over the low-density coronal holes and falls to low values (below 400 km sec^{-1}) when the Earth crosses the band of bright corona.

The inference made during the SKYLAB workshop is that the solar wind speed is always low (down to 300 km sec^{-1}) at *any* neutral line or sector boundary, and that the solar wind speed attains high values ($\cong$750 km sec^{-1}) beyond some distance normal to any neutral line. From this it follows that if a warp in the current sheet is wide enough and deep enough a high-speed solar wind stream will be observed to emanate from the magnetic sector causing the warp. This sector will often contain a coronal hole, but not necessarily. A further consequence of the viewpoint that solar wind comes in two varieties, fast wind and slow wind, is the implied existence of large spatial gradients in the solar wind speed. Values of up to 50 km sec^{-1} per degree of heliographic angle are implied. To speak about a general gradient with latitude would, however, be misleading because the sectors and the streams often cross the equator.

6 GEOMAGNETIC ACTIVITY

The high-speed solar wind causes enhanced geomagnetic activity via a coupling through the interplanetary magnetic field and thus leaves an imprint on the geomagnetic record of the existence of the high-speed stream (e.g. Bartels 1932, Sheeley et al. 1977, Svalgaard 1977). Figure 9 shows the run of geomagnetic activity for the past several years. In this familiar 27-day diagram the large black numbers (C9) indicate high activity. We are near the minimum of the sunspot cycle, as may be seen from the 3-day averages of the sunspot numbers encoded on the left (R9). Several sequences of recurrent storms are readily apparent, some of them with exceptional intensity (especially during 1974). The interplanetary sector structure observed at the Earth during the same time is shown in the right-hand panel of the figure, where white rectangles denote days with dominant positive interplanetary field polarity (i.e. the Earth was north of the current sheet) and black rectangles denote days with negative polarity (the observer being south of the current sheet). Within each magnetic sector, streams (as indicated by high recurrent geomagnetic activity) come and go with a typical lifetime of several solar rotations; the sectors themselves seem to be of a much more permanent nature.

7 COSMIC RAYS

Because of the permanent nature of the sector-related warps in the heliographic current sheet, the band of low-speed solar wind associated

© Annual Reviews Inc. • Provided by the NASA Astrophysics Data System

1978ARA&A..16..429S

Figure 9 Left-hand panel shows geomagnetic activity (C9) and solar activity (R9) since 1972, i.e. on the descending branch of sunspot cycle 20. The data is ordered in 27^{d} Bartels rotations, with larger and heavier symbols denoting the larger activity. On the right is shown the polarity of the interplanetary magnetic field observed at the Earth for the same time interval. The encoding is such that a white rectangle means that the polarity was positive on that day, while a black rectangle signifies a negative polarity. On days with mixed polarity a symbol with vertical bars is used.

© Annual Reviews Inc. • Provided by the NASA Astrophysics Data System

1978ARA&A..16..429S

with the warped sector boundary itself displays a similar warping, which then in connection with solar rotation and the radial expansion of the solar wind leads to regions surrounding the Sun where high-speed plasma interacts with low-speed plasma. In these corotating interaction regions the density and the magnetic field are greatly enhanced, thus providing a possibility of scattering galactic cosmic rays out of the solar system. Gosling et al. (1976) demonstrate the existence of these regions, which become more and more prominent with increasing heliocentric distance. What generates these scattering centers is the speed *differential* between fast and slow solar wind in combination with the warping of the band of closed field lines and solar rotation, which ultimately ensures that solar wind with different speeds will be emitted in the same direction, thus enabling interaction regions to develop. Without any warping of the current sheet that would not happen; the speed profile would be azimuthally symmetric. Because the latitudinal extent of the warps seems to depend on the phase of the sunspot cycle (Svalgaard & Wilcox 1976), a similar variation in the latitudinal extent of plasma interaction regions is expected, possibly thereby modulating the cosmic ray flux into the inner solar system, because interaction regions conceivably act as barriers to cosmic ray propagation. A minimum in cosmic ray flux at Earth is expected when the sectors extend to large heliographic latitudes, i.e. near solar maximum where the polar fields are weak or nonexistent (Svalgaard & Wilcox 1976).

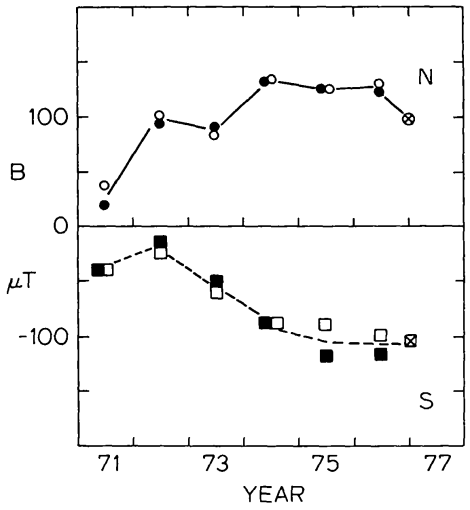

Figure 10 Yearly means of polar field strengths observed at Mt. Wilson (open and filled symbols) and at Stanford Solar Observatory (symbols with crosses) since the polar field reversals of cycle 20. For Mt. Wilson the average fields poleward of 69° (filled symbols) and between 60° and 69° latitude (open symbols) are shown separately for a strip 10° wide in longitude and centered on Central Meridian. For Stanford the average field through a three-minute of arc aperture grazing the poleward limb is plotted. Note: 100 μT = 1 G. (Svalgaard et al. 1978).

© Annual Reviews Inc. • Provided by the NASA Astrophysics Data System

1978ARA&A..16..429S

8 POLAR FIELDS OF THE SUN

A typical magnetic field strength within the solar sector is about 0.5 G or less at this time of the solar cycle (Scherrer et al. 1977). That is not enough to provide the observed interplanetary magnetic flux. A further consequence of the description of the coronal structure that we have reviewed here is that the polar fields of the Sun determine the polarity and presumably also largely the flux of the interplanetary magnetic field away from the solar equatorial plane during the sunspot cycle at times away from sunspot maximum. We may therefore ask: is the polar magnetic flux sufficient to provide the interplanetary flux?

Observations of the polar fields are difficult because they are close to the noise level of most solar magnetographs. Figure 10 shows yearly averages of the line-of-sight magnetic field in the photosphere poleward of about 60° latitude since the latest reversal around 1970. The typical observed flux density is about 1 G. Because the effective latitude of the polar cap above 60° is about 70°, the true average field strength—corrected for line-of-sight foreshortening—should then be about 1 G/cos 70° ≅ 2.5 G. Because of magnetograph saturation (e.g. Stenflo 1973, Svalgaard et al. 1978) this figure is too low by a factor of about two leading to a first crude estimate of the average polar cap field strength of 5 G.

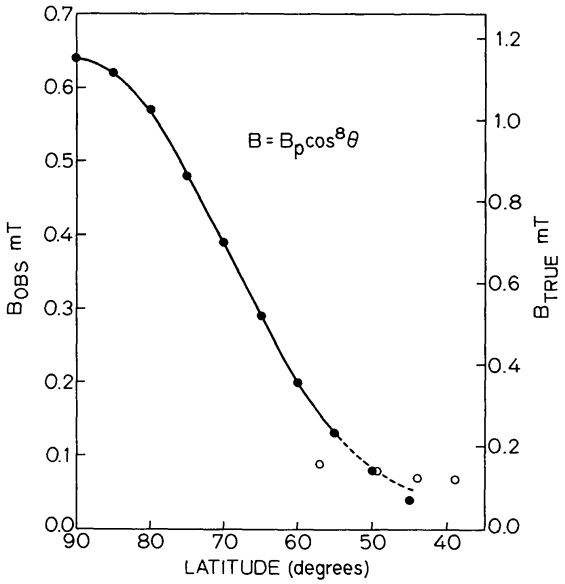

Figure 11 Variation with latitude of the inferred average magnetic flux density between the pole and the polar cap boundary. The ordinate scale on the right reflects the effect of correcting for magnetograph saturation by multiplying the measured flux density by 1.8 (Note: 1 mT = 10 G). A simple analytical expression $B = B_p \cos^8 \theta$ is consistent with the data, where B_p is the field at the pole and θ is colatitude. For the north pole B_p is positive and for the south pole B_p is negative at present. (Svalgaard et al. 1978).

© Annual Reviews Inc. • Provided by the NASA Astrophysics Data System

1978ARA&A..16..429S

At Stanford we have observed the polar field almost on a daily basis since May 1976 (Svalgaard et al. 1978). If the polar fields were uniform (and approximately radial) they would not appear to change in strength during the year as the solar rotation axis tips back and forth towards the Earth by $7\frac{1}{4}°$. We have found that contrary to this, the observed polar fields are subject to a change by about a factor of two during the year. The field appears strongest when the pole is tipped the most towards the observer. A careful analysis of this effect allows us to deduce a plausible variation with latitude of the polar cap fields. The result is shown in Figure 11. We find that the field is strongly peaked towards the very pole reaching almost 12 G and then falling off towards the edge of the polar cap to less than 2 G. The average flux density over the entire polar cap is 6 G and the total flux polewards of 45° is $4 \cdot 10^{14}$ Weber ($4 \cdot 10^{22}$ Mx) for each polar cap. Assuming that the radial field strength at 1 au does not increase with latitude the interplanetary magnetic flux is about $5 \cdot 10^{22}$ Mx in each hemisphere. We see that in fact the polar fields do seem to be sufficient to account for most of the interplanetary flux.

9 CONCLUDING REMARKS

The conclusion reached in the preceding section cannot, of course, hold shortly after sunspot maximum when the polar fields essentially disappear during their reversal. The yearly average magnitude of the interplanetary magnetic field near the Earth is surprisingly constant throughout the solar cycle (King 1976), so that flux must be supplied from some other source near sunspot maximum. Presumably this source is low-latitude magnetic sectors which then must be sufficiently strong in order to supply the flux needed. The present understanding of coronal and interplanetary morphology is based on data acquired during the descending part and the minimum of this one sunspot cycle. It is a challenge to that understanding to apply it to conditions at sunspot maximum and to regions out of the ecliptic. Further observations show to what degree the unified description we have given here needs revision or modification.

ACKNOWLEDGMENTS

It is a pleasure to acknowledge illuminating discussions with our colleagues P. Scherrer, T. Duvall, and K. Schatten. This work was supported in part by the Office of Naval Research under Contract N00014-76-C-0207, by the National Aeronautics and Space Administration under Grant NGR 05-020-559, by the Atmospheric Sciences Section of the National Science Foundation under Grants ATM74-19007 and DES75-15664, and by the Max C. Fleischmann Foundation.

© Annual Reviews Inc. • Provided by the NASA Astrophysics Data System

1978ARA&A..16..429S

Literature Cited

Altschuler, M. D., Newkirk, G. Jr. 1969. *Solar Phys.* 9:131

Antonucci, E. 1974. *Eldo-Cecles/Esro-Cers, Sci. Tech. Rev.* 6:17

Bartels, J. 1932. *Terr. Magn. Atmos. Electr.* 37:1

Bigelow, F. H. 1889. *The Solar Corona.* Washington, D.C.: Smithsonian Inst.

Bohlin, J. D. 1977. In *Coronal Holes*, ed. J. Zirker, pp. 27–69. Boulder, Colo.: Colo. Assoc. Univ. Press. 454 pp.

Duvall, T. L., Jr. 1977. *A Study of large-scale solar magnetic and velocity fields.* PhD thesis. Stanford Univ., Dept. Appl. Phys.

Endler, F. 1971. Zur Wechselwirkung Zwischen Sonnenwind und koronalen Magnetfeldern. Diss. Göttingen Univ., Math.-Nat. Fak.

Gosling, J. T., Hundhausen, A. J., Bame, S. J. 1976. *J. Geophys. Res.* 81:2111

Hansen, S. F., Sawyer, C., Hansen, R. T. 1974. *Geophys. Res. Lett.* 1:13

Howard, R. A., Koomen, M. J. 1974. *Solar Phys.* 37:469

Hundhausen, A. J. 1977. See Bohlin 1977, pp. 255–330

King, J. H. 1976. *J. Geophys. Res.* 81:653

Levine, R. H. 1977. *Ap. J.* 218:291

Pneuman, G. W., Kopp, R. A. 1971. *Solar Phys.* 18:258

Riesebieter, W. 1977. *Dreidimensionale Modellrechnungen zum solaren Wind.* Diss. Tech. Univ. Carolo-Wilhelmina zu Braunschweig, Nat. Fak.

Schatten, K. H., Wilcox, J. M., Ness, N. F. 1969. *Solar Phys.* 6:442

Schatten, K. H. 1971a. *Cosmic Electrodyn.* 11:4

Schatten, K. H. 1971b. *Rev. Geophys. Space Phys.* 9:773

Schatten, K. H. 1976. *Nature* 264:730

Scherrer, P. H., Wilcox, J. M., Svalgaard, L., Duvall, T. L. Jr., Dittmer, P. H., Gustafson, E. K. 1977. *Solar Phys.* 54:353

Schulz, M. 1973. *Astrophps. Space Sci.* 24:371

Sheeley, N. R. Jr., Ashbridge, J. R., Bame, S. J., Harvey, J. W. 1977. *Solar Phys.* 52:485

Stenflo, J. O. 1973. *Solar Phys.* 32:41–63

Smith, E. J., Tsurutani, B. T., Rosenberg, R. L. 1978. *J. Geophys. Res.* 83:717

Svalgaard, L. 1977. See Bohlin 1977, pp. 371–442

Svalgaard, L., Duvall, T. L. Jr., Scherrer, P. H. 1978. *Solar Phys.* In press

Svalgaard, L., Wilcox, J. M. 1975. *Solar Phys.* 41:461

Svalgaard, L., Wilcox, J. M. 1976. *Nature* 262:766

Svalgaard, L., Wilcox, J. M., Duvall, T. L. Jr. 1974. *Solar Phys.* 37:157

Svalgaard, L., Wilcox, J. M., Scherrer, P. H., Howard, R. 1975. *Solar Phys.* 45:83

Vseskhsvjatsky, S. K. 1963. In *The Solar Corona*, ed. J. W. Evans. London: Academic

Waldmeier, M. 1977. *Nature* 265:611

Wilcox, J. M. 1971. *Comm. Astrophys. Space Phys.* 3:133

Wilcox, J. M., Ness, N. F. 1965. *J. Geophys. Res.* 70:5793

Wilcox, J. M., Svalgaard, L. 1974. *Solar Phys.* 34:461

Zirker, J. B. 1977. *Rev. Geophys. Space Phys.* 15:257

© Annual Reviews Inc. • Provided by the NASA Astrophysics Data System